Xu and Zeng
Journal of Engineering and Applied Science (2023) 70:15
https://doi.org/10.1186/s44147-023-00185-w

Journal of Engineering and Applied Science

REVIEWS Open Access

Speed tracking control for electro-hydraulic system considering variable load disturbance

Wenbin Xu[1*] and Le Zeng[2]

*Correspondence:
xwb_770210@126.com

[1] Aeronautical Machinery Manufacturing Department, Airforce Aviation Repair Institute of Technology, Changsha, China
[2] State Key Laboratory of High Performance Complicated Manufacturing, Central South University, Changsha, China

Abstract

Forming speed is one of the key factors affecting metal forming performance. Aluminum in different forming stages need to control different extrusion speed, and withstand different extrusion load. The accuracy and stability of forming speed directly affect the quality of aluminum. Aiming to improve the stability of the forming speed under variable load, the paper established segmented model according to the forming speed and load force conditions. And the unified switching control strategy is proposed based on robust feedback linearized control. In order to improve the robustness of the system, the control law adding compensation items to the variable load disturbance is designed based on the sliding mode control. The boundary layer function is introduced instead of the symbolic function to reduce the system flutter. The proportional derivative control (PD) control, robust control and unified switching control are compared with that of simulation and experiment. The results show that proposed method not only maintains good tracking performance but also has strong robustness under external load disturbance.

Keywords: Electro-hydraulic system, Variable load, Load disturbance, Speed tracking, Multi-model control, Unified switching control

Introduction

The servo valve-controlled asymmetric cylinder system is widely used in the industry, such as in the military, ocean, aerospace and other fields. It has many advantages, such as the compact structure, the small workspace, the large driving capacity, the fast response speed, and the good positioning function [1–3]. However, the high-accuracy control of electro-hydraulic systems is still challenging owing to the highly nonlinear characteristics, the parametric uncertainties, the modeled uncertainties, and the external disturbances [4, 5]. A synchronous control structure with error feedback to solve the problem of insufficient control accuracy of the double cylinder synchronous system for forging hydraulic press [6]. The hybrid fuzzy-PID controller with coupled rules was proposed for position control of an asymmetric hydraulic system [7]. Aiming at the problem of insufficient tracking accuracy caused by nonlinear unknown parameters and unknown external disturbance, an adaptive sliding control method [8], a backstepping design strategy [9], and an adaptive robust controller [10] were presented for an electro-hydraulic system. A cascade controller which was composed of active

disturbance rejection controller and dead zone inverse compensation was designed to improve dynamic performances and position tracking accuracy [11]. Aiming for guaranteeing a better tracking performance in the presence of time-varying uncertainties and external disturbances, a novel backstepping controller based on Levant's differentiator-based disturbance observers had been proposed for a hydraulic system [12]. Aiming for the issue of position tracking control with load-sensing for a valve-controlled cylinder system using speed-controlled fixed displacement pump, a sliding-function-based feedforward controller with a feedback control system was presented to accomplish significant reduction in the input energy [13]. A combination of load sensing technology to regulate the valve control system was used to overcome the problem of low energy efficiency in the operation of the hydraulic press valve control system [14]. Focusing on the position control of low-velocity servo controlled electro-hydraulic actuator system in order to increase the system productivity, an efficient sliding mode control was designed based on the selection of appropriate sliding surface and control law to overcome the nonlinearities and uncertainties caused by friction and internal leakages [15]. In order to avoid wrinkling, an adaptive simulation approach integrated with a fuzzy control algorithm was used to optimize the loading path of hydroforming a T-shaped tube [16]. Aiming at the problems of low power recovery and large heat release of the conventional pump-controlled system free forging hydraulic press, a fast hydraulic forging press with open variable pump-controlled system was proposed to achieve a great energy-saving advantage [17]. An adaptive sliding mode fault-tolerant controller was designed to improve fault-tolerant control ability and control accuracy of heavy-duty hydraulic press under the condition of actuator fault [18]. For a class of multi-cylinder hydraulic presses with overdrive characteristics , a new sliding mode fault-tolerant dynamic allocation method based on disturbance observer was proposed, as showed strong robustness regardless of whether a specific fault occurs in a single hydraulic cylinder or multiple hydraulic cylinders [19]. A nonlinear parallel control algorithm is developed for an electro-hydraulic actuator to improve the velocity tracking performance for a valve-pump parallel controlled electro-hydraulic actuator under uncertainties and disturbance [20]. A novel robust backstepping control strategy was introduced to achieve high-accuracy tracking performance for electro-hydraulic servo systems without velocity information in the presence of uncertainties and disturbances [21]. Forming speed is one of the key factors affecting the forming performance. In the process of metal deformation, the quality of the product is closely related to the speed of forming, especially under the variable load. In order to obtain high-quality extrusion products, forming speed should be as far as possible to be maintained continuously stable, and to avoid fluttering. In this paper, a unified switching control strategy is proposed to improve the speed tracking accuracy by considering the variable load disturbance of the electro-hydraulic system, remaining the forming speed as stable as possible, so as to obtain high-quality products.

Main text

This paper is organized as follows: "System modeling" section presents the studied electro-hydraulic system. The unified switching control strategy based on robust

feedback linearized control, and the system stability analysis are introduced in "Control design" section. "Simulation and experiment" section contains the simulation and experiment results. The conclusions is provided in "Results and discussion" section.

System modeling

The valve-controlled electro-hydraulic system is illustrated in the Fig. 1. A_A, A_B are the piston areas, V_A, V_B are the volumes of the cylinder ports, p_A, p_B are the pressures at the cylinder ports, q_A, q_B are the oil inlet flow of the cylinder ports, P_s is the output pressure of the pump, P_o is the return pressure of oil, m is the load mass (including piston mass), F_L is the forming load force, and x is the piston displacement.

The kinetics model

The driving force of the hydraulic system is composed of the system pressure of the two chambers, the viscous resistance of the medium and the inertia force of the moving parts. The equation of the motion for the piston is written as

$$F = P_A A_A - P_B A_B - b_c \dot{x} - m\ddot{x} \tag{1}$$

where b_c is the load viscous damping coefficient.

During the motion of the electro-hydraulic system at a given reference speed, the forming load force is composed of the friction force and the deformation resistance, which is balanced with the driving force.

$$F_L = F_f + F_\sigma = -F \tag{2}$$

where F_f is the friction force, F_σ is the deformation resistance.

According to Eqs. (1-2),the system kinetics model is expressed as follows:

$$A_A p_A - A_B p_B = m\ddot{x} + b_c \dot{x} - F_\sigma - F_f \tag{3}$$

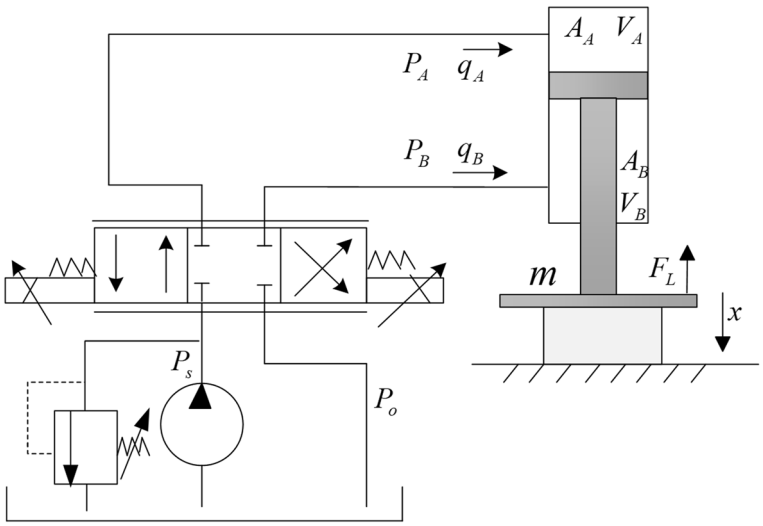

Fig. 1 Structure diagram of the valve-controlled electro-hydraulic system

The flow model

The equations of the flow through the proportional servo valve can be written as follows:

$$q_A = \begin{cases} C_d w x_v \sqrt{\frac{2}{\rho}(p_s - p_A)} & x_v \geq 0 \\ C_d w x_v \sqrt{\frac{2}{\rho} p_A} & x_v < 0 \end{cases} \tag{4}$$

$$q_B = \begin{cases} C_d w x_v \sqrt{\frac{2}{\rho} p_B} & x_v \geq 0 \\ C_d w x_V \sqrt{\frac{2}{\rho}(p_s - p_B)} & x_v < 0 \end{cases} \tag{5}$$

The equations of the flow through the hydraulic cylinder can be written as follows:

$$q_A = \begin{cases} A_A \dot{x} + C_i(p_A - p_B) + C_e P_A + \frac{V_{A0} + A_A x}{\beta_e} \cdot \dot{p}_A & x_v \geq 0 \\ A_A \dot{x} + C_i(p_B - p_A) - C_e P_A + \frac{V_{A0} - A_A x}{\beta_e} \cdot \dot{p}_A & x_v < 0 \end{cases} \tag{6}$$

$$q_B = \begin{cases} A_B \dot{x} + C_i(p_A - p_B) - C_e P_B - \frac{V_{B0} - A_B x}{\beta_e} \cdot \dot{p}_B & x_v \geq 0 \\ A_B \dot{x} + C_i(p_A - p_B) + C_e P_B - \frac{V_{B0} + A_B x}{\beta_e} \cdot \dot{p}_B & x_v < 0 \end{cases} \tag{7}$$

where x_v is the servo valve spool displacement; C_d is the flow coefficient of proportional valve; w is the opening degree of proportional valve; ρ is the density of hydraulic oil; C_i is the internal leakage coefficient in hydraulic cylinder; C_e is the external leakage coefficient in hydraulic cylinder; V_{A0} and V_{B0} are the volumes of the cylinder ports as the hydraulic cylinder in the middle position; β_e is the effective bulk modulus of the hydraulic oil.

The multistate model of the system

The segmentation of the load

The metal forming process is the result of the combination of deformation resistance and forming speed. The essence is the electro-hydraulic speed servo control under time-varying load force, which maintains the desired speed. Based on relationship between forming speed and load force, the forming process can be segmented, as shown in Fig. 2. The numbers of segment can be determined by the variation law of load force.

where $S_1 \sim S_n$ are the segments, $v_1 \sim v_n$ the forming speeds; $F_{L1} \sim F_{Ln}$ the load force.

The multistate model based on the segmentation of the load

The state variables is defined as $x = [x_1\ x_2\ x_3\ x_4]^T = [x\ \dot{x}\ p_A p_B]^T$. Based on that, the state-space equation of the system can be expressed as follows:

$$\begin{cases} \dot{x} = f_i(x,t) + g_i(x,t) \cdot u \\ y = h_i(x) = x_2 \end{cases} \tag{8}$$

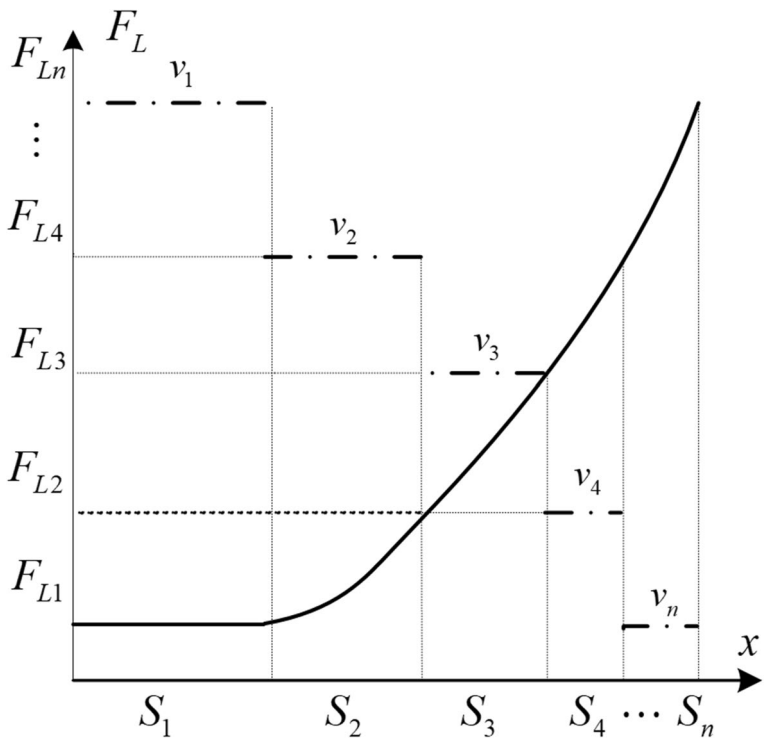

Fig. 2 System segmenting model

$$f_i(x,t)=\begin{bmatrix} x_2 \\ 1/m\cdot\left(A_B\left(\varepsilon x_3-x_4\right)-F_{fi}\left(x_2\right)-F_{\delta i}\right) \\ \beta_e/V_A\left(x_1\right)\cdot\left(-A_A x_2\right) \\ \beta_e/V_B\left(x_1\right)\cdot\left(A_B x_2\right) \end{bmatrix}, g_i(x,t)=\begin{bmatrix} 0 \\ 0 \\ \beta_e/V_A\left(x_1\right)\cdot B_v\sqrt{\Delta\left(x_3\right)} \\ -\beta_e/V_B\left(x_1\right)\cdot B_v\sqrt{\Delta\left(x_4\right)} \end{bmatrix}, i=1,2\cdots,F_{\delta i}$$

where: is the deformation resistance in the corresponding state, $F_{fi}(x_2)$ is the friction force, $\mathrm{V}_A(x_1), V_B(x_1)$ are the working volumes of the cylinder, $\varepsilon=\frac{A_A}{A_B}$, $\Delta(x_3)=\begin{cases} p_s-x_3 & x_v\geq 0 \\ x_3-p_0 & x_v<0 \end{cases}$, $\Delta(x_4)=\begin{cases} \mathrm{x}_4-p_0 & x_v\geq 0 \\ p_s-x_4 & x_v<0 \end{cases}$, $B_v=C_d w\sqrt{\frac{2}{\rho}}$.

From the expression of $\mathbf{f}_{\mathrm{i}}(\mathbf{x},t)$, It can be seen that the deformation resistance in different stages of the forming is inconsistent, equivalent to one forming condition of the electro-hydraulic system. The multi-models of the system can be constructed by establishing the submodel of each condition.

Control design

The structure of the switching control

The state-space equation of the system can be expressed as the Eq. (9).

$$\begin{aligned} \dot{x}\left(t\right) &= A_\sigma x(t)+B_\sigma u(t) \\ y(t) &= C_\sigma x(t) \end{aligned} \tag{9}$$

where: A_σ is $n \times n$matrix,B_σ is $n \times 1$ matrix,C_σ is $1 \times n$ matrix.

Assumed the system meets the following conditions:

(1) For all $i \in \Lambda, 0 \le k \le n-2, C_i A_i^k B_i = 0$;
(2) For all $j \in \Lambda, C_i A_i^{n-1} B_i = C_j A_j^{n-1} B_j = \gamma \ne 0$;
(3) For all $\tau \in \Lambda, \left(C_1 A_1^n, \cdots C_\tau A_\tau^n\right) \in I\tau(G_1, \cdots G_\tau)$.

where: Conditions (1) and (2) indicate that the output is only a state-dependent function for any subsystem. Condition (3) indicates that $C_i A_i^n$ can be reconstructed by $\sum_{j=0}^{n-1} C_i A_i^j$, that is $C_i A_i^n x = \sum_{j=0}^{n-1} l_j C_i A_i^j x$.

If the control law shown in Eq.(10) is selected, the system has a unified control structure, and the system is stable [22].

$$u = \frac{1}{\gamma}\left(y^{(n)} - \sum_{j=0}^{n-1} l_j y^{(j)}\right) \tag{10}$$

where γ is a positive constant.

Assumed $\dot{e}_{\sigma(t),i} = e_{\sigma(t),i+1} = y^{i+1}, e_{\sigma(t),1} = y = C_{\sigma(t)}x$, then the follow equation can be obtained from Eq. (9)–Eq. (10).

$$\dot{e}_{\sigma(t)} = \begin{pmatrix} 0 & 1 & \cdots & 0 \\ \vdots & \vdots & \ddots & \vdots \\ 0 & 0 & \cdots & 1 \\ 0 & 0 & \cdots & 0 \end{pmatrix} e_{\sigma(t)} + \begin{pmatrix} 0 \\ \vdots \\ 0 \\ C_{\sigma(t)} A_{\sigma(t)}^n x + C_{\sigma(t)} A_{\sigma(t)}^{n-1} B_{\sigma(t)} u \end{pmatrix} \tag{11}$$

where $e_{\sigma(t)} = \left[\, e_{\sigma(t),1} \;\; e_{\sigma(t),2} \;\; \cdots \;\; e_{\sigma(t),n} \,\right]^T$.

For the Eq. (11), the control law is expressed as

$$u = \frac{1}{\gamma}\left(-\sum_{j=0}^{n-1} l_j y^{(j)} - \sum_{j=1}^{n} k_j y^{(j)}\right) \tag{12}$$

where $k_j \in R$ and its value is set to ensure that the polynomial $k_1 + k_2 s + \cdots + k_n s^{n-1} = 0$ be Hurwitz. According to Eq. (11)–Eq. (12), The following expression can be obtained as the Eq. (13).

$$\dot{\boldsymbol{e}}_{\sigma(t)} = \boldsymbol{A}\boldsymbol{e}_{\sigma(t)} \tag{13}$$

where $A = \begin{pmatrix} 0 & 1 & \cdots & 0 \\ \vdots & \vdots & \ddots & \vdots \\ 0 & 0 & \cdots & 1 \\ -k_1 & -k_2 & \cdots & -k_n \end{pmatrix}$.

Defined that $T_i = \left[C_i \; C_i A_i C_i \; A_i^{n-1}\right]^T$, then the Eq. (13) can be converted as follows:

$$\dot{\boldsymbol{y}} = \boldsymbol{T}_{\sigma(t)}^{-1} \boldsymbol{A} \boldsymbol{T}_{\sigma(t)} \boldsymbol{y} \tag{14}$$

For the electro-hydraulic system shown in Eq. (8), the output of the system is only related to the state of the system and there is an independent input-output relationship for any

subsystem. Therefore, a unified switching control structure can be applied to the system. Through differential homeomorphism transformation, the Eq. (8) can be converted as the Eq. (15).

$$\dot{\boldsymbol{x}} = \begin{pmatrix} 0 & 1 & \cdots & 0 \\ \vdots & \vdots & \ddots & \vdots \\ 0 & 0 & \cdots & 1 \\ 0 & 0 & \cdots & 0 \end{pmatrix} \boldsymbol{x} + \begin{pmatrix} 0 \\ \vdots \\ 0 \\ \alpha(\boldsymbol{x}) + \beta(\boldsymbol{x})u \end{pmatrix} \tag{15}$$

where $\alpha(x) = -\left(\varepsilon^2 \frac{F}{V_A(x_1)} + \frac{E}{V_B(x_1)}\right) \cdot \frac{A_B^2}{m} x_2 - \dot{F}_{Li}/m, \beta(x) = \frac{A_B B_V}{m}\left(\varepsilon \frac{E}{V_A(x_1)} \cdot \sqrt{\Delta x_3} + \frac{E}{V_B(x_1)} \cdot \sqrt{\Delta x_4}\right)$

The control law is expressed as

$$\alpha(\mathbf{x}) + \beta(\mathbf{x})u = K\mathbf{x} \tag{16}$$

where K is the gain of the control.

From Eq. (15), the following result can be obtained.

$$\dot{\boldsymbol{x}} = \begin{pmatrix} 0 & 1 & \cdots & 0 \\ \vdots & \vdots & \ddots & \vdots \\ 0 & 0 & \cdots & 1 \\ -k_1 & -k_2 & \cdots & -k_n \end{pmatrix} \boldsymbol{x} = K\boldsymbol{x} \tag{17}$$

For each submodel, the control law is expressed as

$$\alpha_i(\mathbf{x}) + \beta_i(\mathbf{x})u = K_i\mathbf{x} \tag{18}$$

Then, the system structure can be expressed as

$$\dot{x}_i = \begin{pmatrix} 0 & 1 & \cdots & 0 \\ \vdots & \vdots & \ddots & \vdots \\ 0 & 0 & \cdots & 1 \\ -k_{1i} & -k_{2i} & \cdots & -k_{ni} \end{pmatrix} \boldsymbol{x} = K_i x \tag{19}$$

The switching controller

For any submodel, it can be written as

$$f_i(x,t) = \begin{bmatrix} x_2 \\ 1/m \cdot \left(A_B(nx_3 - x_4) - F_{Li}(x)\right) \\ E/V_A(x_1) \cdot (-A_A x_2) \\ E/V_B(x_1) \cdot (-A_B x_2) \end{bmatrix} \tag{20}$$

Relative order calculating

Given $\nabla h(x) = [0\ 1\ 0\ 0]$, $\nabla h(x)$ is the gradient of $h(x)$, $g_1(\mathbf{x}) = E/V_A(x_1) \cdot B_V\sqrt{\Delta(x_3)}$, and $g_2(\mathbf{x}) = -E/V_B(x_1) \cdot B_V\sqrt{\Delta(x_4)}$. By the definition of the relative order, the Eq. (8) has the relative order r.

If the relative order $r=1$, then $L_g h(x) = [0\ 1\ 0\ 0]\begin{bmatrix} 0 \\ 0 \\ g_1(x) \\ g_2(x) \end{bmatrix} = 0.$

If the relative order $r=2$, then

$$L_f h(x) = [0\ 1\ 0\ 0]\begin{bmatrix} x_2 \\ 1/m \cdot (A_B(\varepsilon x_3 - x_4) - F_{Li}) \\ E/V_A(x_1) \cdot (-A_A x_2) \\ E/V_B(x_1) \cdot (A_B x_2) \end{bmatrix} = 1/m \cdot \Big(A_B(\varepsilon x_3 - x_4) - F_{Li};$$

$$L_g L_f h(x) = \begin{bmatrix} 0\ 0\ \dfrac{\varepsilon A_B}{m}\ \dfrac{-A_B}{m} \end{bmatrix}\begin{bmatrix} 0 \\ 0 \\ g_1(\mathbf{x}) \\ g_2(\mathbf{x}) \end{bmatrix} = g_1(\mathbf{x}) \cdot \frac{\varepsilon A_B}{m} - g_2(\mathbf{x})\frac{A_B}{m} \neq 0.$$

The switching control law

In order to simplify the analysis process, the relative order of the system is selected as 2. Through differential homeomorphism transformation to the Eq. (8), the Eq. (21) can be obtained as follows:

$$\begin{cases} z_1 = h(x) = x_2 \\ z_2 = L_f h(x) = \frac{(A_A x_3 - F_{Li} - A_B x_4)}{m} \end{cases} \tag{21}$$

The Eq. (21) is converted into Brunovsky standard type as

$$\begin{cases} \dot{z}_1 = z_2 \\ \dot{z}_2 = \alpha(\boldsymbol{x}) + \beta(\boldsymbol{x}) \cdot u \\ \dot{\varsigma} = q_i(\varsigma, \boldsymbol{x}) \end{cases} \tag{22}$$

where ς is the internal dynamics of the system and stable [23].

The feedback linearized control law is selected as

$$u = \frac{\nu - \alpha(x)}{\beta(x)} \tag{23}$$

Defined $\nu = \upsilon_d^{(2)} + K_\upsilon e + K_a \dot{e}$, the controller can be designed according to the design method of the linear system.

where $e = \upsilon_d - \upsilon$, υ_d is the desired velocity, K_υ is the feedback coefficients of the velocity error, K_a is the feedback coefficients of the acceleration error, strictly positive, its value configures the poles in the left half-plane.

In order to improve the robustness of the system, the compensation is added on base of on sliding mode control, and the compensate part is expressed as the following.

$$u(t) = \frac{\nu - \alpha(x) - K_i \operatorname{sgn}(s)}{\beta(x)} \tag{24}$$

where s is the sliding mode variable, $\operatorname{sgn}(s)$ is the symbolic function, K_i is the compensation for the uncertain parameters and load disturbance, and speed convergence control.

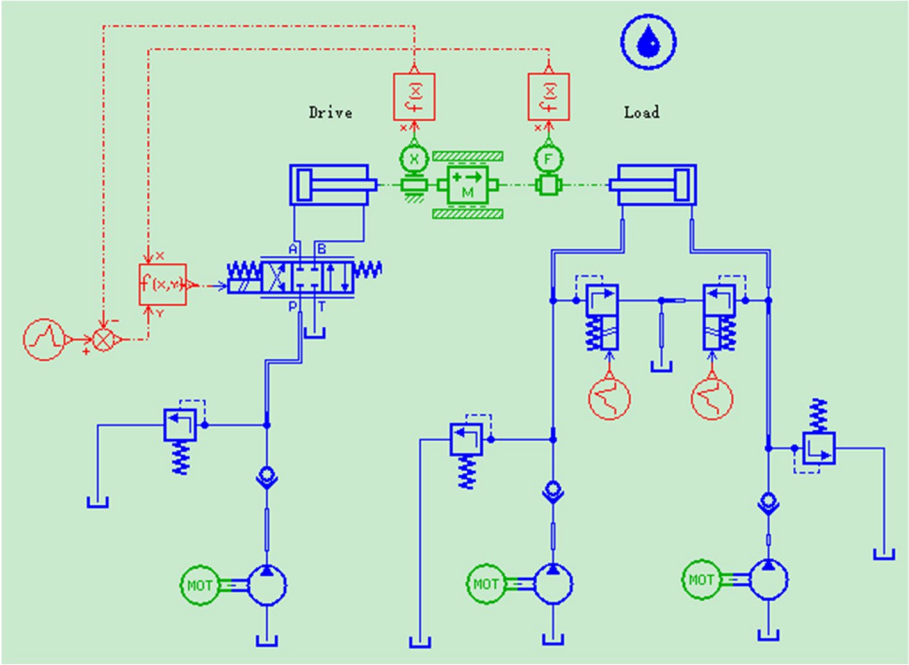

Fig. 3 Simulation model of the system

In order to reduce control energy and the fluctuation of the control law, $K_i \mathrm{sgn}(s) \triangleq \eta_i + K\mathrm{sgn}(s)$, where η_i is the equivalent compensation of variable load, $K\mathrm{sgn}(s)$ is the switch component.

Then, the Eq. (24) can be converted as

$$u(t) = \frac{v - \alpha(x) - \eta_i - K\ \mathrm{sgn}(s)}{\beta(x)} \tag{25}$$

From the Eq. (25), a uniform control structure exists for any subsystem, the difference is that η_i needs to be adjusted according to the subsystem. The boundary layer function $[\mathrm{sgn\ s}] = \begin{cases} \mathrm{sgn}\left(\frac{s}{\Phi}\right), & \left|\frac{s}{\Phi}\right| \geq 1 \\ \frac{s}{\Phi}, & \left|\frac{s}{\Phi}\right| < 1 \end{cases}$ ($\Phi$is the boundary layer thickness) is introduced to replace $[\mathrm{sgn}(s)]$ to reduce the system flutter.

The analysis of the stability

The common Lyapunov function of the system is constructed as $V = \frac{1}{2}s^2, \dot{s} = -K_i[\mathrm{sgn}\ s]$, then $\dot{V} = s \cdot \dot{s} \leq -s^2 - K_i s \cdot [\mathrm{sgn}\ s]$.

In the boundary layer outside, the system is stable as long as $K_i > 0, \dot{V} < 0$. In the boundary layer inside, the system is also stable for $\dot{V} = s \cdot \dot{s} \leq -s^2 - K_i \cdot s[\mathrm{sgn}\ s] = -s^2 - K_i \cdot s^2/\Phi < 0$. According to the Eq. (25), the system is always stable when $K > 0$.

As a conclusion, the common Lyapunov function exists for $K_i > 0$, so the system is stable.

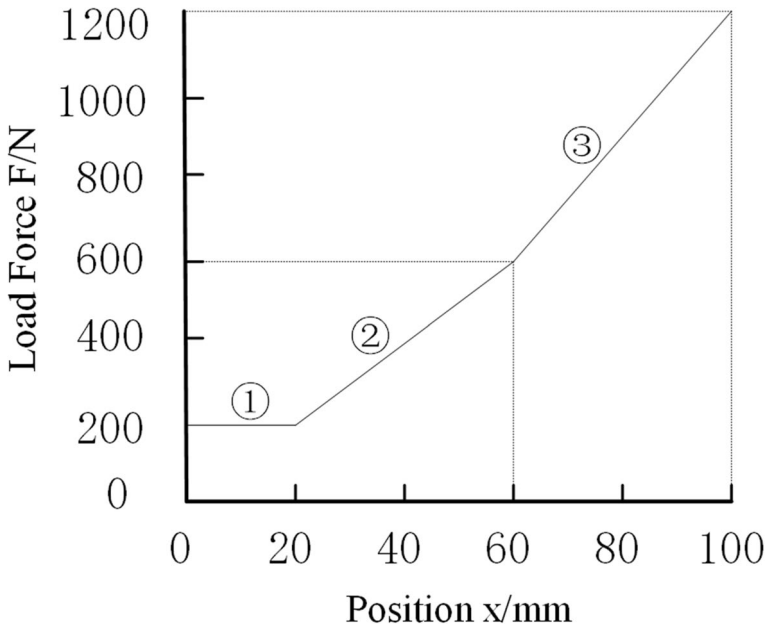

Fig. 4 Simulation load setting

Table 1 Simulation parameters

States	Range/mm	Velocity/m/s	F_L/N
①	0–20	0.03	200
②	20–60	0.02	$200 + 1000(x - 0.02)$
③	60–100	0.01	$600 + 1500(x - 0.02)$

Simulation and experiment

Simulation results

A joint simulation platform of the AMESIM and Simulink is built for the valve-controlled asymmetric cylinder system as the Fig. 3.

The simulation load is shown in Fig. 4. ① indicates no load, ② and ③ indicate two different load states. Piston itinerary is 100 mm, and the specific parameters are listed in Table 1. The unified switching control parameters are as follows: $K_v = 12675$, $K_a = 195$, $\Phi = 200$,$\eta_1 = 100$, $\eta_2 = 150$.

The speed response and errors of electro-hydraulic system through the PD control, the robust control and the unified switching control respectively are shown in Fig. 5. Under condition ①, the steady-state error of the PD control is about 0.5 mm/s, while that of the robust control and the switching control is very small. Under conditions ②② and ③, the steady-state error of the PD control and the robust control increases, while that of the unified switching control remains unchanged. It shows that the unified switching control achieves better speed response performance of electro-hydraulic system under variable load.

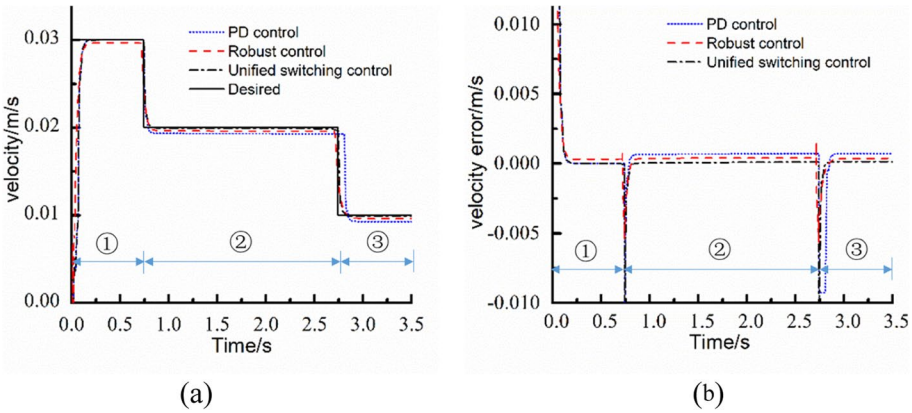

Fig. 5 Simulation result. **a** Speed responses of the system, **b** speed errors

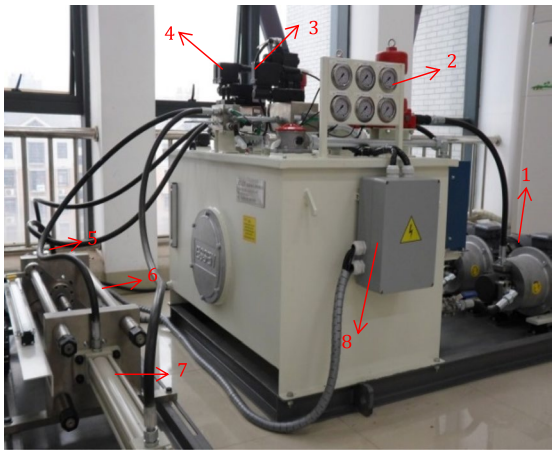

1. Hydraulic pump station
2. indicators
3. Proportional valves
4. Proportional pressure valve
5. Load cylinder
6. Connecting section to the head cylinder
7. Drive cylinder
8. Terminal block

Fig. 6 The experiment structure of the system

Table 2 The hydraulic system parameters

Parameters	Value	Parameters	Value
D_p(L·min^{-1})	20	A_A(m^2)	0.001963
p_s(Mpa)	5	A_B(m^2)	0.001347
C_l(m^3·s^{-1}·Pa^{-1})	1×10^{-12}	L(m)	0.1
β_e(Mpa)	1.4×10^3	M(Kg)	50

Experiment results

Experiment structure of electro-hydraulic system is shown in Fig. 6.

The system parameters of the hydraulic system are listed in the Table 2. The load in the experimental process is shown in Fig. 7. The unified switching control parameters are as follows: $K_v = 32000$, $K_a = 225$, $\Phi = 3200$, $K' = 50$, and $\eta_1 = 100$, $\eta_2 = 200$. The desired speed of the system is 0.01 m/s.

The speed responses of the PD control, the robust control and the unified switching control are compared in Fig. 8. Under the PD control, as the load increases, the

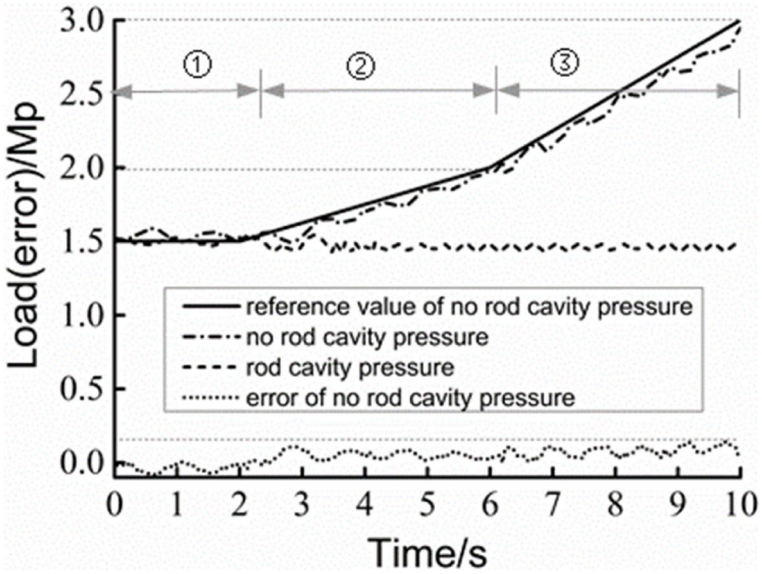

Fig. 7 Experiment load

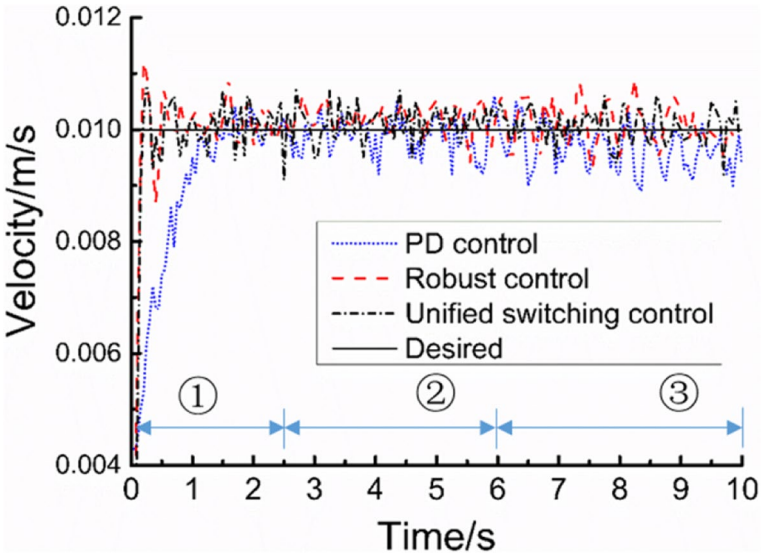

Fig. 8 Speed response under different controls

error increases, and the steady-state reaches 0.001 m/s. Under the robust control, the steady-state error increases with the increase of load, as reaches 0.0005 m/s when under the condition ③. While the steady-state error with the unified switching control remains within 0.0002m/s. It demonstrates that unified switching control can achieve higher speed tracking performance under variable load and is robust to load change.

The system responses of the switching control to different desired speeds are shown respectively in Figs. 9 and 10. The steady-state errors are both about 0.0002 m/s in 0.01 m/s

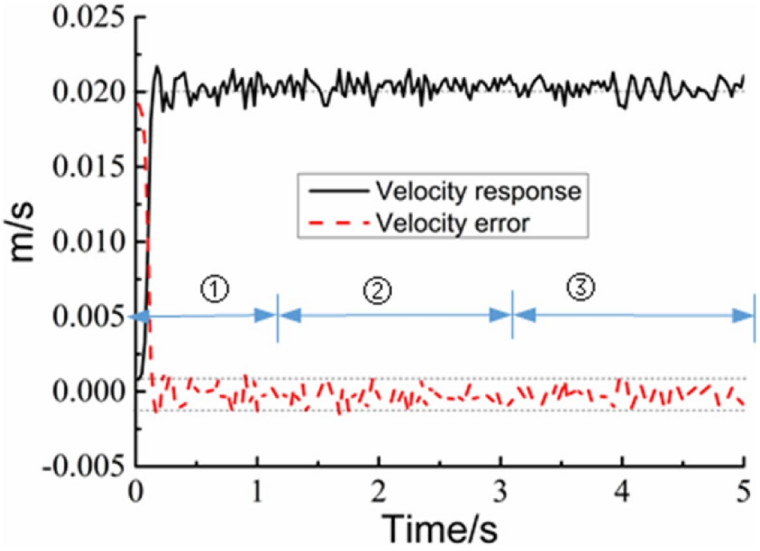

Fig. 9 Speed response under 0.01 m/s

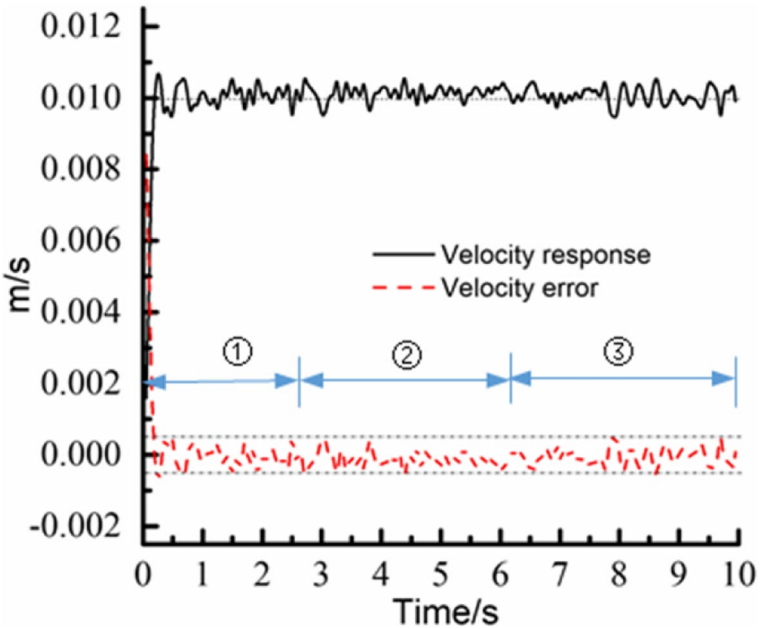

Fig. 10 Speed response under 0.02 m/s

and 0.02 m/s. It demonstrates that the unified switching control has better robustness to the speed change under a certain range of external load.

Conclusions

The control of the electro-hydraulic system due to variable load disturbance is studied to improve the speed control accuracy and robustness of the system. In view of the variable load of the electro-hydraulic system, it is proposed to treat different working conditions as one load state and establish the multistate model of the system. Aiming to improve

the stability of the speed control under variable load, a unified switching control of the electro-hydraulic system is proposed. Simulation and experiment are carried out to compare the response of the PD control and the robust control. The results demonstrate that the unified switching control can effectively suppress the speed tracking problem under variable load disturbance.

Methods/experimental

Velocity was one of the key factors affecting the forming quality. The authors focused on the stability and robustness of the electro-hydraulic system running speed under variable load disturbance. By analyzing the relationship between the operating condition and the speed of the system, the relevant state variables were introduced, the mathematical model of the system was established, and the unified switching control was applied to control the system running state. In the simulation process, the operating speed of the system under different operating conditions was set by simulation and the load forces under different operating conditions were adjusted to obtain the actual output speed of the system, and the speed values of the system under different operating conditions were obtained. The corresponding results were obtained by AEMSIM software. At the same time, the experimental verification was completed through the asymmetric top cylinder experimental platform, which was built with 125MN extruder as the prototype. The relevant experimental data were collected, and the corresponding conclusions were acquired.

Results and discussion

The control of system stability and robustness was explored in the study, which can provide some reference for engineering application. By adopting the unified switching strategy, the stability of the system running speed under different working conditions could be improved with less vibration. However, as the dynamic characteristics of the system were affected by various factors such as the nonlinearity of the system itself, variable load, and variable parameters, the study focused on the variable load, so there was still a certain gap compared with the actual application. The next research will optimize the system model on this basis, and select more realistic parameters through repeated simulation and experiment to further improve the stability and robustness of the system.

Acknowledgements
First and foremost, I appreciate my college who give me a comfortable working and researching atmosphere. Second, I would like to show my deepest gratitude to my supervisor, Prof. Tan Jianping, who has walked me through all the stages of the writing of this thesis. Without his illuminating instruction and patience, this thesis could not have reached its present form. I am also greatly indebted to all my teams who have helped me to develop the fundamental and essential academic competence. My sincere appreciation also goes to all my colleagues, who are my proud of my life. Last but not least, I want to thank all my friends, for their encouragement and support.

Authors' contributions
The manuscript was written through contributions of all authors. And all authors have read and approved the manuscript, which is the case.

Funding
The research was funded by the National Key Basic Research Development Program (2014 CB049400) and The Natural Science Foundation of Hunan Province (2020 JJ7084).

Availability of data and materials
The datasets used or analyzed during the current study are available from the corresponding author on reasonable request.

Declarations

Competing interests
The authors declare that they have no competing interests.

Received: 25 October 2022 Accepted: 16 February 2023
Published online: 03 March 2023

References

1. Liu KL, Li XC, Chen JF (2019) Research on independent metering leveling control system of large hydraulic press, Mechanical Science and Technology for. Aerospace Eng 38(04):522–529
2. Zhao CC, Yang SF, Liu PP (2012) Principle and theoretical analysis of the balancing system for large die forging hydraulic press, China. Mech Eng 48(10):82–89
3. Xu DG, Wu SL, Zhao K (2005) The theoretical analysis and experimental study about the position servo system of valve controlled single-rod cylinder, Chinese. Hydraul Pneumat 06:35–39
4. Wang X, Tao JF, Zhang FR, Wu Y (2016) Unidirectional proportional pump controlled asymmetric cylinder control method based on predictive control. J Shanghai Jiaotong Univ 50(05):696–701
5. Komsta J, van Oijen N, Antoszkiewicz P (2013) Integral sliding mode compensator for load pressure control of die-cushion cylinder drive. Control Eng Pract 21(05):708–718
6. Li SY (2020) Research on the synchronous control system of two cylinders for forging hydraulic press, Chinese. Hydraul Pneumat 347(07):99–105
7. Çetin Ş, Akkaya AV (2010) Simulation and hybrid fuzzy-PID control for positioning of a hydraulic system. Nonlinear Dyn 61(03):465–476
8. Guan C, Pan S (2008) Adaptive sliding mode control of electro-hydraulic system with nonlinear unknown parameters. Control Eng Pract 16(11):1275–1284
9. Sirouspour MR, Salcudean SE (2000) On the nonlinear control of hydraulic servo-systems. IEEE 2(12):1276–1282
10. Zou X, Liu XY, Zhao HM (2021) Adaptive robust control of electro-hydraulic load simulator based on extended observer. J Univ Shanghai Sci Technol 43(06):551–559
11. Wang LX, Zhao DX, Liu FC (2021) ADRC for electro-hydraulic position servo systems based on dead-zone compensation. China Mech Eng 32(12):1432–1442
12. Nguyen MH, Dao HV, Ahn KK (2021) Active disturbance rejection control for position tracking of electro-hydraulic servo systems under modeling uncertainty and external load. Actuators 10(02):20
13. Cho SH, Noskievič P (2012) Position tracking control with load-sensing for energy-saving valve-controlled cylinder system. J Mech Sci Technol 26(02):617–625
14. Li KH, Jiang GY, Zhu DB (2022) Throttling automatic control load sensing hydraulic system of hydraulic press and its simulink simulation. Forg Stamp Technol 47(03):169–173
15. Tony Thomas A, Parameshwaran R, Sathiyavathi S (2022) Improved position tracking performance of electro hydraulic actuator using PID and sliding mode controller. IETE J Res 68(03):1683–1695
16. Teng B, Li K, Yuan S (2013) Optimization of loading path in hydroforming T-shape using fuzzy control algorithm. Int J Adv Manuf Technol 69(08):1079–1086
17. Yao J, Ren XH, Cao XM, Zhao JS (2017) Experimental study on energy consumption characteristics of fast hydraulic forging press with open variable pump-controlled system. China Mech Eng 28(04):462–470
18. Xu JX, Ma H (2020) Adaptive sliding mode fault-tolerant control of actuator for heavy-duty hydraulic press. Forg Stamp Technol 45(04):140–147
19. Jia C, He HC, Dong EZ (2021) Dynamic allocation of sliding mode fault tolerance of hydraulic press based on disturbance observer. J Huazhong Univ Sci Technol (Nat Sci Edition) 49(08):33–39
20. Li M, Shi W, Wei J (2019) Parallel velocity control of an electro-hydraulic actuator with dual disturbance observers. IEEE Access 07:56631–56641
21. Nguyen MH, Dao HV, Ahn KK (2022) Extended sliding mode observer-based high-accuracy motion control for uncertain electro-hydraulic systems. Int J Robust Nonlinear Control 32(10):1–20
22. Zheng G, Boutat D, Barbot JP (2010) "On Uniform Controller Design for Linear Switched Systems", Nonlinear Analysis. Hybrid Syst 4(01):189–198
23. Yang J, Tan JP (2014) Robust feedback linearization control of valve controlled asymmetric cylinder system. J Huazhong Univ Sci Technol (Nat Sci Edition) 42(02):106–110

Publisher's Note